Numerical Analysis of Flat Receiver Placement of Parabolic Dish Collector for Solar Energy Application

B. Kumar[*,1]**, J. N. Roy**[1]**, M. K. Das**[2]

[1]School of Energy, Science and Engineering, Indian Institute of Technology Kharagpur - 721302, India
[2]Department of Mechanical Engineering, Indian Institute of Technology Kharagpur - 721302, India
Email: brajeshkumar998@gmail.com, jnroy@atdc.iitkgp.ac.in, manab@mech.iitkgp.ac.in

Abstract- **Available solar energy is in diluted form; therefore, we need a reflector to collect solar thermal energy. Parabolic dish collector is a good source for medium and high-temperature ranges. It is used to increase the concentrated heat flux at the receiver surface. Due to the high concentration ratio temperature of the localized surface of the receiver is very high. Therefore, to reduce the localized point heat flux on the flat receiver surface, we disperse the concentrated flux over the entire surface using the optimization of the receiver placement. In existing design criteria, the receiver is placed at a focal point called a focal plane, but with the help of numerical simulation of the parabolic dish collector using COMSOL Multiphysics®, we replaced the receiver over the optimal plane, where heat flux gets distributed up to the entire surface without hampering the efficiency of the system. We design a 1 kW output system of a parabolic dish collector for numerical solution. The average available beam radiation is taken 700 W/m2 for 6 hours a day for simulation. The projected diameter of the collector is 7.08 m2, and the receiver diameter is varied from concentration ratio 80 to 120, and the rim angle is varying from 15° to 90°. It is observed that a 45° rim angle is more efficient, and localized heat flux is overcome when the receiver is placed at the optimal plane, and efficiency losses are less than 2%.**

Keywords- Parabolic Dish Collector, Heat flux, Beam Radiation, Rim Angle

1. INTRODUCTION

Solar energy provides an unlimited, clean, and renewable source of energy. The main drawback is that this is a very dilute source of energy. In solar thermal-based systems, a large collector area is required for harnessing solar energy, increasing the overall cost of the solar system. Solar parabolic dish reflector systems are used to focus incident solar radiation into a small region resulting in very high heat flux. This heat is further converted into electrical energy, thermal energy, or chemical energy. The availability of solar irradiance and heat flux is studied by various authors [1–4]. There are several computational methods available to predict the concentration ratio. Jeter [5] proposed a semi-analytical method in which the concentration ratio is computed using the integration of the intensity distribution over the concentrator surface. Various authors [6–7] also study the solar concentrator system for energy supply and management.

The issue of local heating is still a concern. Generally, the receiver is placed at the focal plane. This results in the surface energy per unit time to be very high at the center only. This causes local heating reducing the life of the system. A different way of flux distribution optimization at the receiving surface using a rim angle and the optimal plane distance is required. A different approach has been presented in this paper. The receiver is placed in such a way that all reflected ray falls on the entire surface of the receiver. This reduces local heating and local stress. An equation has been developed for calculating the optimal plane for any projected diameter, rim angle (15° to 90°), and the concentration ratio (60 to 120). COMSOL Multiphysics® and PVWatts® simulators have been used for this study, and the calibrations, as well as validations, are done using available literature data.

2. SYSTEM CONFIGURATION AND DESIGN PARAMETERS

A schematic of the solar dish reflector is shown in Fig. 1. The incoming ray converges at the receiver which is mounted at the focal plane. Rim angle (ϕ) [8] is the angle subtended by the perpendicular line drawn through the center of the receiver to the edge of the reflector.
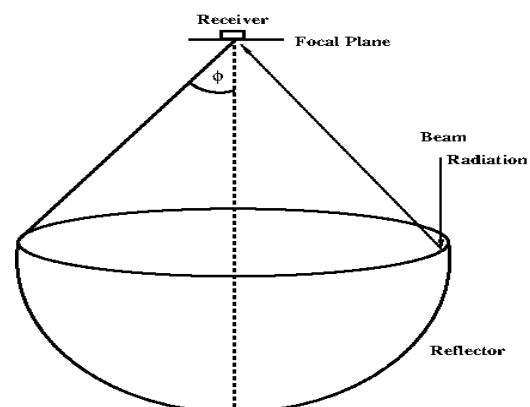
Fig. 1 Schematic of parabolic dish reflector.

The dish collector system has been designed for 1 kW output for 6 hours a day to investigate the effect of rim angle and focal plane distance. This can be scaled up for the larger system and various applications for industry. The assumption for the design is based on the availability of local-global beam radiation. The simulations are done for six different places in India. Table 2 shows the availability of global beam radiation (Gbn) of different places in India. The software PVWatts® simulator [9] is used for calculating beam radiation of different areas. The average beam radiation intensity of six locations in India is 702.3 W/m2, which is very close to 700 W/m2, reported by Funk (2000) [10].

Table 2: Beam radiation availability of different places in India.

Place	Total daily beam radiation availability for 6hr a day (W/m^2) [9]
Kharagpur	640
Kolkata	599
Mumbai	788
Delhi	622
Ahmadabad	796
Nagpur	769

Collector geometric concentration (C_g), which is defined in Eq. 1, has been taken as 60, 80, 100, and 120 for this design.

$$C_g = A_p / A_b \qquad (1)$$

where C_g is the geometric concentration ratio, A_P is the projected aperture area of the reflector (m^2), and A_b is the receiver area or absorber area (m^2). Various losses such as optical loss, pumping loss, thermal loss, and reflector loss have been considered to estimate system output. Table 3 shows the design parameter of the solar dish collector. The estimated area of reflector, absorber, and focal point is given in Eq. 2-5.

$$A_p = Q / (\eta_o \times \eta_{th} \times \eta_p \times \eta_{ref} \times G_{bn}) \qquad (2)$$

$$A_b = A_p / C_g \qquad (3)$$

$$f = \left(\sqrt{A_p \times \frac{4}{\pi}} \right) / \left(4 \left(\frac{1}{sin\phi} - \frac{1}{tan\phi} \right) \right) \qquad (4)$$

$$A_{ap} = 4\pi f^2 \frac{sin^2\phi}{1 + cos\phi} \qquad (5)$$

where f is the focal length of the parabolic reflector (m), A_{ap} is the total surface area of the reflector (m^2). From Eq. 2-4, aperture area, receiver area, and focal length are calculated. Table 3 shows the various parameters used for designing the solar dish collector. The projected area of the reflector is 7.08 m^2. The receiver diameter varies with respect to the

geometrical concentration ratio, which is shown in Table 4.

Table 3: Various parameters used for designing the solar dish collector.

Parameter	Value
η_o [11]	0.7
η_{th} [11]	0.4
η_p [12]	0.8
η_{ref} [11]	0.9
G_{bn} (W/m^2) [10]	700
Operating time (hr)	6

Table 4: Receiver radius for different geometric concentration ratio.

Concentration Ratio	Radius of Receiver (cm)
60	19.4
80	16.7
100	15
120	13.7

3 MATHEMATICAL MODEL AND GOVERNING EQUATIONS

The primary geometrical relationship between the reflecting source and receiver is shown in Fig. 2. The differential area elements on the surface of the reflector are *dc*, whereas the optimal plane of the receiver is at *P*. The surface normal at the reflector and focal plane is n$_r$ and n, respectively. The following angles are defined: $\delta = \angle F\, dc\, P$; $\theta_c = \angle P\, dc\, n_r$; $\theta = \angle dc\, P\, n$.
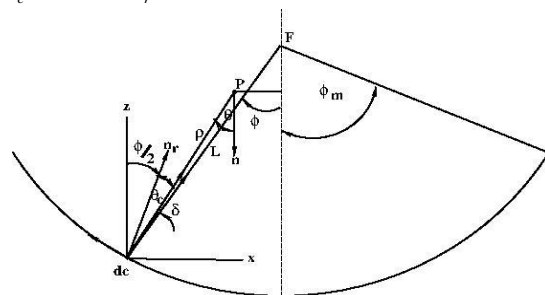
Fig. 2 Geometrical relation between receiving point P displaced from the focal point.

The concentration ratio is a function of the radial position in the receiving plane. Integrating over all azimuthal angles, the concentration ratio at the receiver can be found as given in Eq. 6.

$$C_r(r) = \frac{1}{G_{bn}} \int_\Omega \frac{I\, cos(\theta)\, cos(\theta_c)}{|\rho|^2} dA_r \qquad (6)$$

$$I(\delta) = \begin{cases} G_{bn} / (\pi\, sin^2(s)) & \delta \le s \\ 0 & \delta > s \end{cases} \qquad (7)$$

$$q = C_r(r)G_{bn}$$

$$(8)$$

where I is the radiant intensity (W/m^2 steradian), Ω denotes surface integration over the collector surface (steradian), G_{bn} is the incident solar flux (W/m^2), S is maximum solar half-angle (4.65 mrad) [14] and dA_r is a differential area element on the surface of the reflector (m^2).

4 SIMULATION AND VALIDATION

The incident flux on the surface of the receiver is computed using a ray optics module in COMSOL Multiphysics®. The illuminated surface boundary condition from the reflector to the receiver is used. For numerical simulation, some assumptions are made. It has been assumed that all incoming rays are parallel to each other. Ray propagation is computed uniformly throughout the material. The available normal beam radiation $G_{bn} = 700$ W/m^2.

Heat flux density at the receiver is simulated for different rim angles and different focal plane distances. The simulation domain of the solar dish reflector and receiver is shown in Fig 3. The isometric view and side view of the complete domain are shown in Fig 3. The projected area of the reflector is kept constant, i.e., 7.08 m^2. The radius of the receiver (r_r) is varied for different concentration ratios (60, 80, 100, and 120), and the rim angle (ϕ) is varied from 15° to 90°. The surface slope error (σ) is kept at 1.8 mrad [13]. The absorption coefficient (α) is kept 0 and 0.1.

Table 5: Focal length for different rim angle

Rim angle (ϕ)	Focal length (m)
15°	5.7
30°	2.8
45°	1.8
60°	1.3
75°	0.98
90°	0.76

Four different sets of triangular mesh are generated using the mesh generation module. Coarse grids are considered on the reflector, and fine grids are considered on the receiving surface. The first set of grids 62642, the second set of grids 125356, the third set of grids 258628 and the fourth set of grids 558996 are taken for simulation. The computational domain, along with grids, is shown in Fig. Grid independence variation of flux distributions is shown in Fig. The abscissa shows the radial distance in the x-y plane, and the ordinate shows the average flux distribution. The percentage variation in average flux distribution is shown in Table 6. Grid sets of 125356 and 258628

show identical flux distribution, and deviation is less than 5%, but the grid set of 62642 and 558996 show significant variation at the periphery of the receiver. Since a set of grid 62642 and 558996 has more than 5% deviation, an optimal grid 125356 is used for further computation.
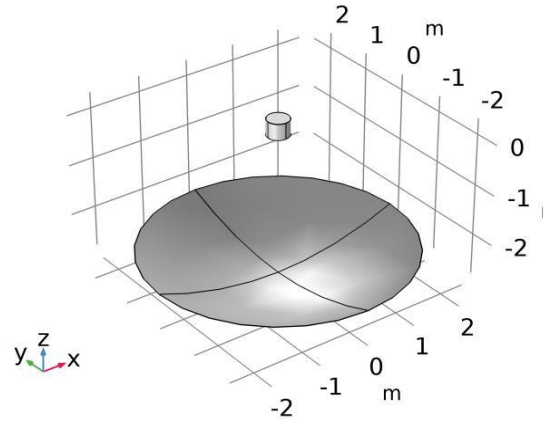
Fig 3 Simulation domain of solar dish reflector and receiver for 30° rim angle
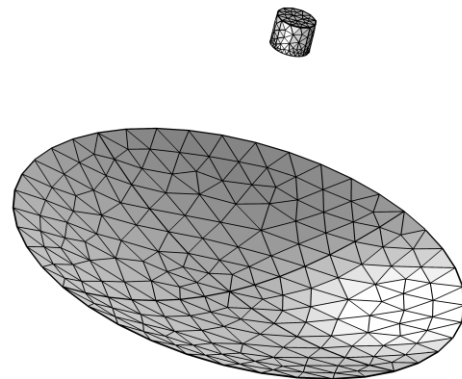
Fig.4 Grid for computational domain.
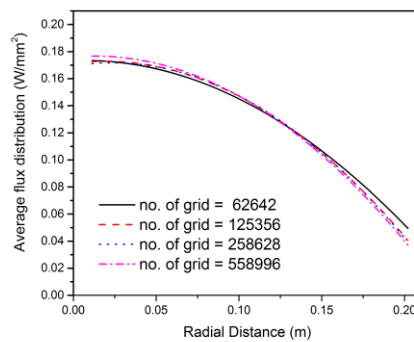
Fig. 5 Grid independence study.

Computational models are validated with the published result of Jeter (1986) [5] and Shuai *et al.* (2008) [6]. Validation of present computational work with the different authors is shown in Fig. 4. Different absorption coefficients $\alpha = 0$ and 0.1 show good agreement with the published benchmark.

Table 6: Percentage variation in average flux distribution when increasing the number of grids.

No. of grids	Average flux near the center (W/mm^2)	% Deviation from mean	Average flux near the periphery (W/mm^2)	% Deviation from mean
62642	0.173	-0.3	0.049	16.6
125356	0.173	-0.3	0.041	-2.3
258628	0.171	-1.4	0.040	-4.7
558996	0.177	2.02	0.038	-9.5
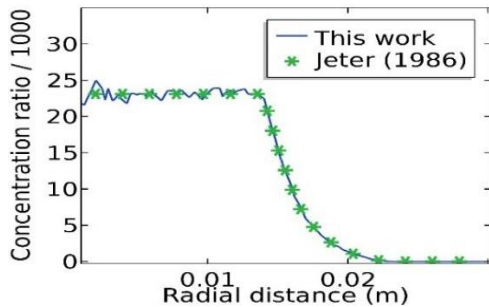
(a) Variation of concentration ratio at α = 0 with Jeter (1986).
(b) Variation of flux distribution at α = 0.1 with Shuai et al. (2008).
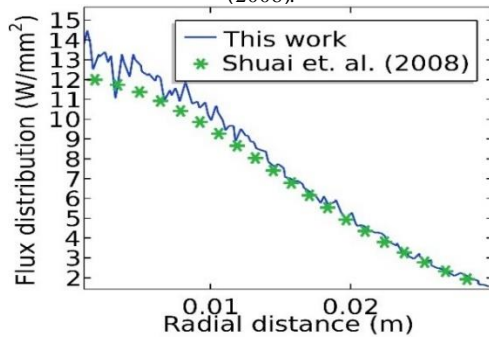
Fig. 4 (a) and (b) Validation of present computation at α = 0 and 0.1.

5. RESULTS AND DISCUSSIONS

5.1 Optimization of rim angle and concentration ratio for flux distribution

The effect of rim angle and concentration ratio for flux distribution is shown in Figures 7 and 8, where the receiver is kept at the focal plane and the optimal plane. The rim angle is varied from 15° to 90° at 15° intervals. The surface and radial flux distribution of concentration ratio 80 is shown in Figures 7 and 8. From figure 7, it is clear that the flux density at the center is very high, which can result in the degradation of material used due to high temperature. However, when the receiver is placed at an optimal plane, then flux density is evenly distributed up to the entire surface resulting in reduced local temperature. However, if the receiver is placed at an optimal plane, then for the lower rim angles (15^0 to 75^0), the flux density is evenly distributed up to the entire surface; this is not so for a rim angle above 75°. In this case,

the flux density is not evenly distributed up to the whole receiving surface. Flux density for rim angle at 90° has point concentration even it is placed at an optimal plane. Therefore, a rim angle above 75° is unsuitable unless and until high localized flux density is required for the specific application.
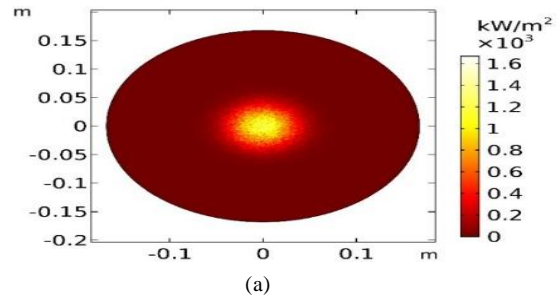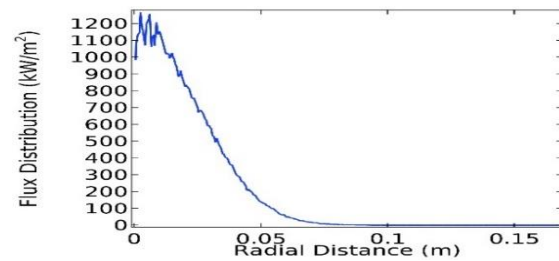
Fig. 7.(a) Surface flux and (b) radial flux, distribution on the receiver at rim angle ($\phi = 15°$) when the receiver is placed at the focal plane.
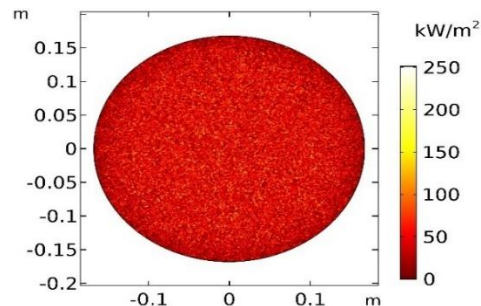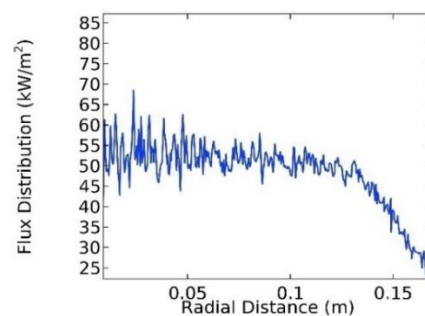
Fig. 8 (a) Surface flux and (b) radial flux, distribution on the receiver at rim angle ($\phi = 15°$) when the receiver is placed at an optimal plane.

Table 7 represents surface energy per unit time for different concentration ratios when the receiver is placed at an optimal plane. The maximum surface energy per unit time (4.45 kJ/s) is received at the focal plane. When the receiver is placed at a 45° rim angle, it reaches maximum surface energy per unit time even when placed on an optimal plane. At a rim angle of 45°, surface energy per unit time is maximum, and flux density is evenly distributed up to the entire receiving surface. The maximum loss of surface energy per unit time is 0.004% to 2%, which is negligible. For 15° rim, angle loss is up to 12%, which is significant, reducing overall system efficiency. It is clear (Table 7 and Figure 9) that the rim angle 15° is less efficient, and the rim angle 45° is most appropriate.

Table 7: Surface energy per unit time for different concentration ratios and rim angles when the receiver is placed at optimal plane.

C_r	Surface energy per unit time (kJ/s)					
	Different rim angle at an optimal plane					
	(15°)	(30°)	(45°)	(60°)	(75°)	(90°)
60	4.08	4.33	4.45	4.36	4.35	4.30
80	4.02	4.29	4.43	4.34	4.33	4.25
100	3.95	4.26	4.40	4.33	4.30	4.24
120	3.90	4.24	4.38	4.32	4.30	4.22
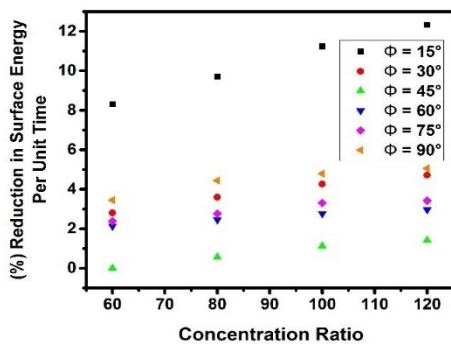
Fig. 9 Percentage reduction in surface energy per unit time when the receiver is placed at the optimal plane.

5.2 The relation between the optimal plane and focal plane

The receiver is placed at the focal point where all reflected rays from the dish reflector are collected at the receiver's centre, which is considered the focal plane (f_p). If the receiver is placed so that all reflected ray is collected up to the periphery of the receiver, this is considered an optimal plane (o_p).

Table 8 gives the distance of the receiving surface for the focal plane and the optimal plane of different concentration ratios. Equation 9 gives the relation between the optical plane and the focal plane. Variation in the focal plane and optimal plane for different concentration ratios and different rim angles

is shown in Figure 10. It is clear (Figure 10) that deviation in the optimal plane is more for smaller rim angles, whereas for the higher rim angle focal plane and the optimal plane falls on the same point. It is also noticed that deviation in the optimal plane for a low concentration ratio is more, but deviation in the optimal plane is less for a higher concentration ratio. For concentration ratio 60 to 120, the optimal plane overlaps each other.

$$o_p = f - \frac{d}{2\sqrt{C_r}} \times \frac{cos(\phi)}{sin(\phi)} \qquad ` \quad (9)$$

Table 8: Distance of focal plane and optimal plane for different concentration ratio and rim angle.

ϕ (°)	f_p (m)			o_p (m)	
		C_r (60)	C_r (80)	C_r (100)	C_r (120)
15	5.69	4.97	5.07	5.13	5.18
30	2.79	2.46	2.50	2.53	2.56
45	1.81	1.61	1.64	1.66	1.67
60	1.29	1.18	1.20	1.21	1.21
75	0.98	0.92	0.93	0.93	0.94
90	0.75	0.75	0.75	0.75	0.75
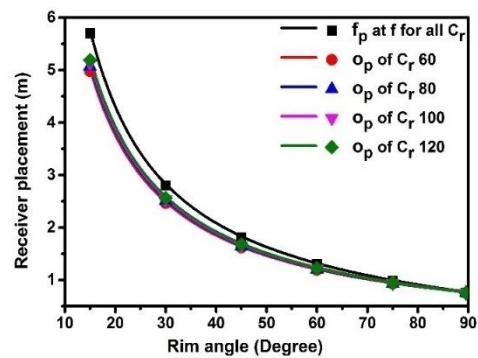
Fig. 10: Receiver placement for different rim angle of different concentration ratio.

The optimal plane for any focal length (f) and projected diameter (d) of the dish reflector can be directly calculated from Eq. 9 for different rim angles $15° \le \phi \le 90°$ and concentration ratios $60 \le Cr \le 120$

6. CONCLUSION

A new approach has been used to design a dish collector to increase the life of the system without sacrificing efficiency. The dish collector system has been designed for 1 kW output for 6 hours a day. This can be scaled easily for industrial applications. The projected area of the dish collector is 7.08 m². The rim angle (ϕ) is varied from 15° to 90°. The concentration ratio is varied for 60, 80, 100, and 120. It is established that the rim angle of 45° is 8% more efficient than the rim angle of 15°. The surface energy per unit time (4.45 kJ/s) is maximum at 45° rim angle, and surface energy per unit time (4.08 kJ/s)

is minimum at rim angle 15°. When the receiver is placed at the optimal plane, the dispersion of energy density is up to the periphery, and the maximum loss is less than 2% in the case of a 45° rim angle. When the rim angle is beyond 75°, the energy density is not distributed up to the periphery, and energy density is high at the center because, beyond the 75° rim angle, the optimal plane and focal plane coincides with each other. An equation has been developed to calculate the optimal plane using rim angle and concentration ratio directly. This applies to a wide range of rim angles 15° to 90° and a concentration ratio of 60 to 120. Further integration of the receiver with latent heat storage for industrial and domestic applications will reduce CO_2 emissions and increase energy savings. It also leads society and nations towards sustainable development.

7. ACKNOWLEDGMENTS

8. REFERENCES

[1] Howell J R, Menguc M P, Siegel R (**2010**) Thermal Radiation Heat Transfer, *5th ed. CRC press.*

[2] Morciano M, Fasano M, Secreto M, et al (**2016**) Installation of a Concentrated Solar Power System for the Thermal Needs of Buildings or Industrial Processes. *Energy Procedia* 101:956–963.

[3] Muthu G, Shanmugam S, Veerappan A R (**2014**) Solar parabolic dish thermoelectric generator with acrylic cover. *Energy Procedia* 54:2–10.

[4] Nixon J D, Dey P K, Davies P A (**2010**) Which is the best solar thermal collection technology for electricity generation in north-west India? Evaluation of options using the analytical hierarchy process. *Energy* 35:5230–5240.

[5] Jeter S M (**1986**) The distribution of concentrated solar radiation in paraboloidal collectors. *J Sol Energy Eng* 108:219–225.

[6] Shuai Y, Xia X L, Tan H P (**2008**) Radiation performance of dish solar concentrator/cavity receiver systems. *Sol Energy* 82:13–21.

[7] Santosh B B, Rohit K and Inderjeet S (**2020**) Development of a novel two-stage parabolic dish collector-receiver system for efficiency improvement. *Energy Sources, Part A: Recovery, Utilization, and Environmental Effects* 2020:1-32.

[8] Sup B A, Zainudin M F, Zanariah S A T, et al (**2015**) Effect of rim angle to the flux distribution diameter in solar parabolic dish collector. *Energy Procedia* 68:45–52.

[9] https://pvwatts.nrel.gov/pvwatts.php.

[10] Funk P A (**2000**) Evaluating the International Standard Procedure for Testing Solar Cookers and Reporting Performance. *Sol Energy* 68:1–7.

[11] Mohammed I L (**2012**) Design and Development of a Parabolic Dish Solar Water Heater. *Int J Eng Res Appl* 2:822–830.

[12] Ulanicki B, Kahler J, Coulbeck B (**2008**) Modeling the Efficiency and Power Characteristics of a Pump Group. *J Water Resour Plan Manag* 134:88–93.

[13] Johnston G (**1998**) Focal region measurements of the 20 m² tiled dish at the Australian National University. *Sol Energy* 63:117–124.